Title	Comparisons of physical imaging properties among three kinds of imaging plates used in photostimulable phosphor systems for dental radiography
Author(s)	Nishikawa, K; Ooguro, T; Kuroyanagi, K
Journal	Bulletin of Tokyo Dental College, 43(1): 23-30
URL	http://hdl.handle.net/10130/303
Right	

Bull. Tokyo dent. Coll., Vol. 43, No. 1, pp. 23～30, February, 2002

Original Article

COMPARISONS OF PHYSICAL IMAGING PROPERTIES AMONG THREE KINDS OF IMAGING PLATES USED IN PHOTOSTIMULABLE PHOSPHOR SYSTEMS FOR DENTAL RADIOGRAPHY

KEIICHI NISHIKAWA, TOSHIKI OOGURO* and KINYA KUROYANAGI

Department of Oral and Maxillofacial Radiology, Tokyo Dental College, 1-2-2 Masago, Mihama-ku, Chiba 261-8502, Japan

* *Department of Oral and Maxillofacial Radiology, Kanagawa Dental College, 82 Inaoka-cho, Yokosuka, Kanagawa 238-8580, Japan*

Received 16 November, 2001/Accepted for Publication 18 January, 2002

Abstract

The purpose of this study was to compare the physical imaging properties of three kinds of imaging plates (IPs) used with two photostimulable phosphor systems for dental radiography: HR-V, used with the Digora, BAS-SR, and ST-V, used with the DenOptix for intraoral radiography and panoramic radiography, respectively. Sensitivity to X-ray, gradient, modulation transfer function (MTF), noise power spectrum (NPS), noise-equivalent quanta (NEQ), and detective quantum efficiency (DQE) were compared. All imaging plates were read using the DenOptix scanner with inactive automatic range control (ARC). The scanning resolution was set at 300 dpi. Decay of image information by room light was also compared at inactive and active ARC settings. BAS-SR showed the lowest sensitivity, the lowest gradient, the highest MTF, and the highest NPS. ST-V showed the highest sensitivity, the highest gradient, the lowest MTF, and the lowest NPS. HR-V was the second best for all imaging properties examined in this study. NEQ and DQE of BAS-SR were lowest, and those of ST-V were highest at low spatial frequencies. However, BAS-SR showed relatively constant NEQ and DQE while those of ST-V decreased remarkably at high spatial frequencies. NEQ and DQE of HR-V were the second best at low spatial frequencies and the best at high spatial frequencies. Therefore, we concluded that HR-V has the best imaging properties for dental radiography among three kinds of IPs evaluated in this study. However, the light decay speed of image information with HR-V was remarkably faster than with BAS-SR. To adopt HR-V for a system with which IPs are treated in an ordinary room, the light decay should be taken into account.

Key words: Dental radiography—Photostimulable phosphor system—Imaging plate—Imaging property—Light decay

---

This study was presented in part at the 12th International Congress of Dentomaxillofacial Radiology, Osaka, June 30, 1999.

INTRODUCTION

Major digital dental radiographic systems can be classified into two groups according to their X-ray sensors: charge-coupled device (CCD)-based systems and photostimulable phosphor systems. Most systems are CCD-based. There are only three photostimulable phosphor systems available on the market worldwide: Digora® (Orion Co./Soredex, Helsinki, Finland), DenOptix™ (Dentsply International, Inc./Gendex Dental X-ray Div., Des Plaines, IL, USA), and a series of products manufactured by Digident, Ltd. (Nesher, Israel). Each of these systems uses a different type of imaging plate. The performance of these systems is strongly dependent on the imaging plate. In this study, we compared the physical imaging properties of three types of imaging plates used in the Digora and DenOptix systems.

MATERIALS AND METHODS

The imaging plates (IPs) used in this study were HR-V, BAS-SR and ST-V. All of them are manufactured by Fuji Photo Film Co., Ltd. (Tokyo, Japan). HR-V is used with the Digora. BAS-SR and ST-V are used with the DenOptix for intraoral radiography and panoramic radiography, respectively. Sensitivity to X-ray, gradient, modulation transfer function (MTF), noise power spectrum (NPS), noise-equivalent quanta (NEQ), and detective quantum efficiency (DQE) were measured and compared. Decay of image information by room light was also compared. All IPs were read using the DenOptix scanner. The IP of the Digora and that of the DenOptix for panoramic radiography were reshaped to fit the intra-oral IP holder of the scanner carousel. In evaluating the physical imaging properties, the function of the automatic range control (ARC) available with the DenOptix[7] was inactivated (ARC OFF). In evaluating light decay of image information, the experiments were performed with both inactive and active ARC settings (ARC OFF and ARC ON). All other parameters for automatic image manipulation were inactivated. The scanning resolution was set at 300 dots per inch (dpi).

The X-ray source was a Coronis 20 dental X-ray unit (Asahi Roentgen Industry, Inc., Kyoto, Japan). This unit uses single-phase full-wave rectification and has a nominal focal spot of $0.8 \times 0.8\,mm^2$. Total filtration is 2.0 mm aluminum equivalent. The tube voltage and the tube current were fixed at 70 kVp and 10 mA, respectively, throughout the study. Only the exposure time was varied. Long focus-IP distance of 170 cm was used to eliminate the effect of focal spot size, heel effect, and the effect of slanting X-rays. Radiation exposure was measured with a calibrated dosimeter RAMTEC 1000D (Toyo Medic Co., Ltd., Tokyo, Japan).

Obtained images were analyzed using a Windows 95 (Microsoft Co., Redmond, WA, USA) based personal computer and two general-purpose application software programs, a free image processing and analysis application, Scion Image Beta3b (Scion Co., Frederick, MD, USA), and a spreadsheet application, Excel 97 (Microsoft Co.).

1. Sensitivity to X-ray

IPs were uniformly exposed by X-ray at different exposures. Three images were acquired for each exposure. Obtained images were imported to the Scion Image. The region of interest (ROI) of 64×64 pixels was set at the center of each image, and the mean pixel value (luminance value; the lower the pixel value, the darker the image) was calculated using a function of the Scion Image. An ensemble average of the mean pixel values for the three images was obtained. A characteristic curve of each IP was generated to compare the sensitivity to X-ray.

2. Gradient

Gradient value, which is defined as the difference in pixel value against the small increment of the logarithm of the exposure dose, was calculated using an approximation formula for each characteristic curve. Gradient curves of each IP were generated against loga-

rithm of exposure.

3. Modulation transfer function (MTF)

The analysis method of Fujita *et al.*[3] was employed to measure the presampling MTF of each IP along the scanning direction of the scanner. A 10μm slit camera (Nuclear Associates, Inc., Carle Place, NY, USA) was used to obtain slit images. The slit was positioned on IPs and slightly angled from the true perpendicular line to the scanning direction in order to provide optimal sampling data for the line spread function (LSF). Obtained images were imported to the Scion Image. The ROI of 128×128 pixels was set at the position which included each slit image. Slit image data were stored as a text data file. The file was read on an Excel worksheet. The composite LSF was constructed, and the tails of the LSF were extended by exponential extrapolation. The presampling MTF was determined from the Fourier transform of the LSF. The fast Fourier transform method was employed. The MTF of each IP was obtained as the average of the presampling MTFs calculated from three slit images.

4. Noise power spectrum (NPS)

The technique reported by Giger *et al.*[5] was employed for calculating the digital NPS of each IP. The ROI of 256×256 pixels was set at the center of each image with uniform exposure, which was used for generating characteristic curves, using the Scion Image. The image data within the ROI were stored as a text data file, which was read on an Excel worksheet. Each ROI image was scanned by a hypothetical scanning slit with a width of 1 pixel and a length of 32 pixels. Eight slit tracings were extracted from one ROI image. Because three images were prepared for the same exposure, 24 slit tracings could be used for calculating the NPS of each IP for each exposure. To eliminate the background trend, each slit tracing was smoothed using polynomial curve fitting. The smoothed data were subtracted from the slit tracing to yield the noise tracing with a zero mean value. The NPS was determined from the Fourier transform of the noise tracing. The square of the modulus of the Fourier transform of the noise tracing was calculated. Spectral data were divided by the length of the tracing and multiplied by the appropriate slit length. The spectra computed from all of the noise tracings were averaged and smoothed using a curve-fitting method to obtain the digital NPS in terms of pixel values. The digital NPSs in terms of exposures, $W_{\Delta E/E}(f)$, were then calculated using the gradient values of the characteristic curves, as given by

$$W_{\Delta E/E}(f) = W_{PV}(f) / (\log_{10} e \cdot G)^2,$$

where $W_{PV}(f)$ is the NPS in terms of pixel values, G is the gradient at the mean pixel value of the noise image, and f represents spatial frequency. The NPS was obtained for several radiation exposures within the dynamic range of each IP.

5. Noise-equivalent quanta (NEQ) and detective quantum efficiency (DQE)

The NEQ spectrum is derived from the presampling MTF and the NPS using the following equation:

$$NEQ(f) = [MTF_{ps}(f)]^2 / W_{\Delta E/E}(f),$$

where $MTF_{ps}(f)$ represents the presampling MTF. The DQE spectrum is computed as

$$DQE(f) = NEQ(f) / Q,$$

where Q is the mean number of incident X-ray photons per unit area. This number was calculated from the measured values of exposure and half value layer using the data table for photon fluence per röentgen[6]. The NEQ and the DQE were calculated for several radiation exposures within the dynamic range of each IP.

6. Light decay of image information

IPs were uniformly exposed by X-ray at the maximal exposure within the dynamic range of each IP. They were left in an ordinary room and exposed to room light (287 lx). After exposure to room light for a designated number of seconds, they were read using the scanner. Obtained images were imported to the Scion Image. The ROI of 64×64 pixels was set at

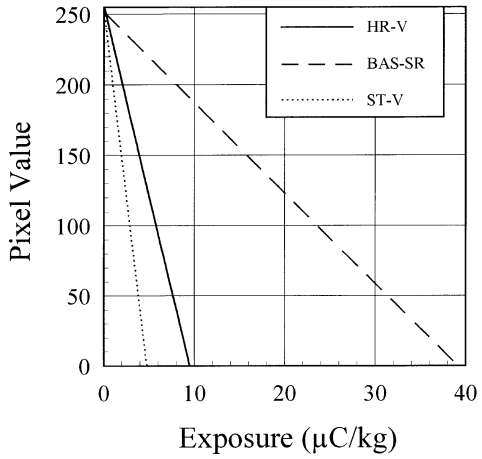

Fig. 1 Characteristic curve

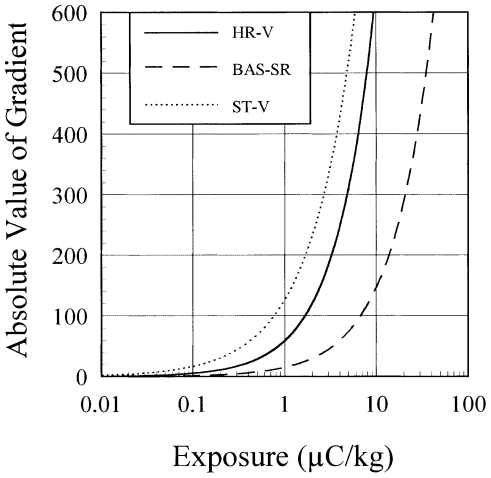

Fig. 2 Gradient curve

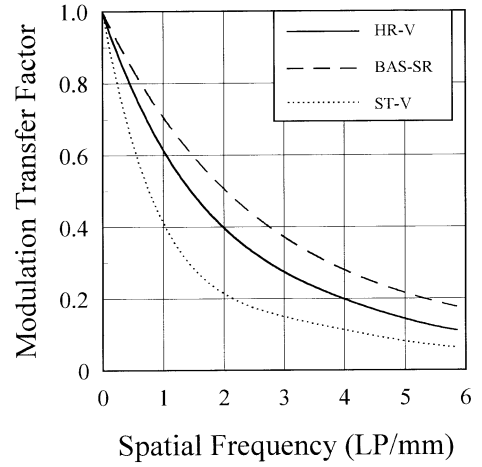

Fig. 3 Presampling MTF

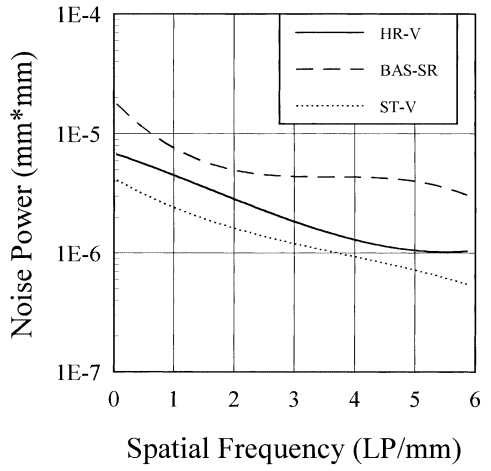

Fig. 4 Digital NPS of each IP at exposure of 3.3μC/kg

the center of each image, and the mean pixel value was calculated. To investigate the noise level, the root mean square (RMS) value (the standard deviation of pixel values within the ROI), which is a simple index that represents the noise level as one figure, was also calculated. Changes in pixel value and RMS value with both the ARC OFF and ARC ON settings were compared among the IPs.

RESULTS

1. Sensitivity to X-ray

Fig. 1 shows the characteristic curve for each IP. The exposure on the horizontal axis is expressed in linear scale. The ST-V showed the highest sensitivity and that of the BAS-SR was lowest. The dynamic range of each IP was quite different.

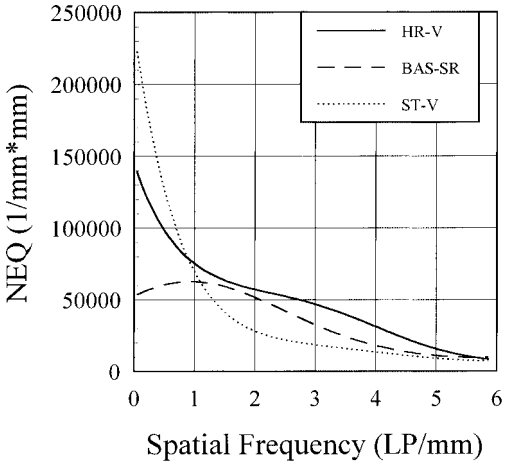

Fig. 5 NEQ of each IP at exposure of 3.3μC/kg

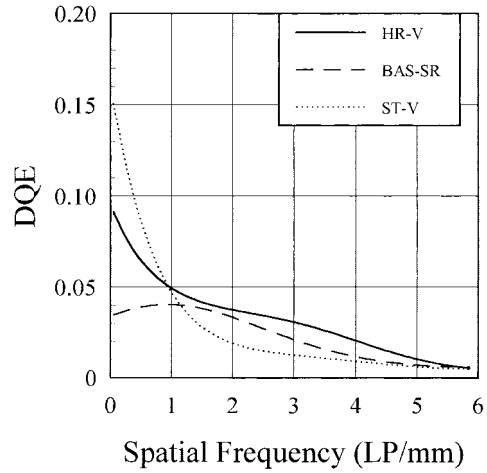

Fig. 6 DQE of each IP at exposure of 3.3μC/kg

2. Gradient

The gradient curves against exposure in logarithmic scale are shown in Fig. 2. The vertical axis represents the absolute value of the gradient because the pixel value decreased with increases in exposure and the gradient itself showed a negative value. The gradient value of ST-V was highest, and that of BAS-SR was lowest against the same exposure.

3. Modulation transfer function (MTF)

The presampling MTF of each IP is shown in Fig. 3. MTF of the BAS-SR was highest, and that of the ST-V was lowest.

4. Noise power spectrum (NPS)

It was very difficult to directly compare the digital NPS of each IP for the same exposure because the three IPs had quite different dynamic ranges. Only the spectra obtained under one exposure condition could be compared in this study. Fig. 4 shows the digital NPS of each IP for exposure of 3.3μC/kg. The fluctuation of exposure for each IP was within 2 %.

The NPS of ST-V showed the lowest noise level at every spatial frequency. The noise level of BAS-SR was highest.

5. NEQ and DQE

Fig. 5 shows the results of comparison of NEQ obtained at exposure of 3.3μC/kg. NEQ of ST-V decreased remarkably with increases of spatial frequency while BAS-SR showed relatively constant NEQ. NEQ of ST-V was the highest up to a spatial frequency of 0.9 LP/mm and the lowest at a spatial frequency above 1.1 LP/mm. NEQ of HR-V was the second highest at a spatial frequency below 0.9 LP/mm and the highest above 0.9 LP/mm.

Fig. 6 shows the results of comparison of DQE. Because the DQE of each IP was calculated for the same exposure, the figures were similar to those of NEQ. The maximal DQEs of HR-V, BAS-SR, and ST-V were approximately 0.09, 0.04, and 0.15, respectively.

6. Light decay of image information

Fig. 7 (a)–(d) indicate decay of image information by room light. Changes of pixel value and RMS value with ARC OFF are shown in (a) and (b). The BAS-SR showed the slowest increase of pixel value, and the ST-V was fastest. With the setting of ARC ON, the pixel values of all IPs were kept almost constant against exposure time to room light within 180 seconds. However, the RMS values were remarkably increased. The BAS-SR

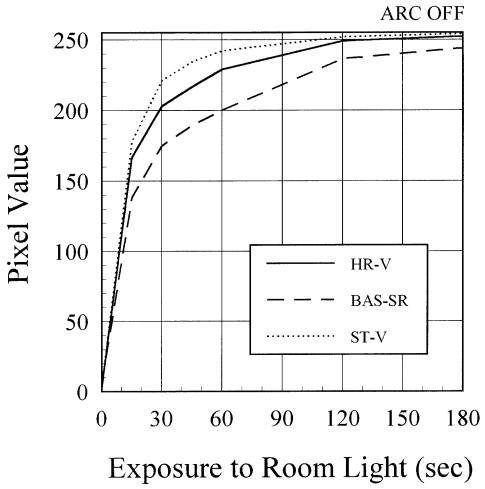

(a) change in pixel value with ARC OFF

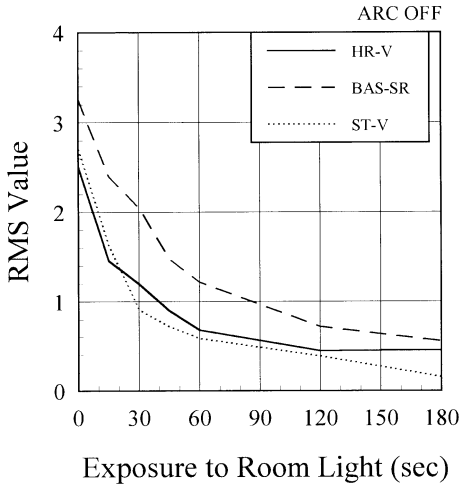

(b) change in RMS value with ARC OFF

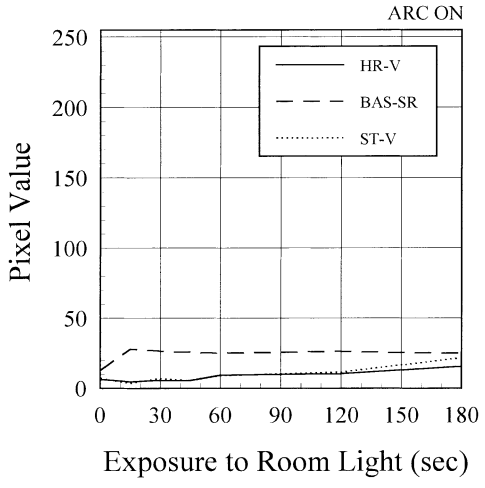

(c) change in pixel value with ARC ON

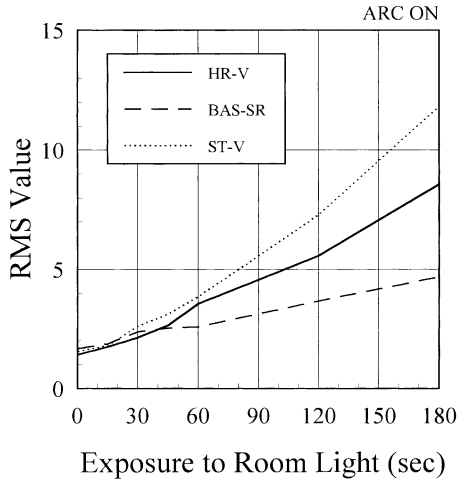

(d) change in RMS value with ARC ON

Fig. 7 Decay of image information by room light

showed the slowest increase, and the ST-V, the fastest.

DISCUSSION

The BAS-SR used with the DenOptix for intraoral radiography was superior in the MTF to the other IPs. However, the sensitivity of the BAS-SR was quite inferior. Low sensitivity causes low detection efficiency of X-rays and results in large noise, low NEQ, and low DQE. On the other hand, the ST-V used with the DenOptix for panoramic radiography showed the worst MTF, although the sensitivity was best. Therefore, NEQ and DQE of the ST-V decreased remarkably at the high spatial frequencies. The HR-V used with the Digora

showed the second best sensitivity, the second best MTF, and the second best NPS. There were no major flaws that decreased the image quality. As a result, NEQ and DQE of HR-V were the second best at low spatial frequencies and the best at high spatial frequencies.

There are no reports that have compared NEQ or DQE among different storage phosphor systems for dental radiography or different IPs used with phosphor systems for dental radiography. Borg *et al.*[1] compared the Digora and the DenOptix systems. The inherent combinations, the Digora scanner with HR-V and the DenOptix scanner with BAS-SR, were evaluated at their default settings. Their results showed that the DenOptix had a higher MTF and higher noise than the Digora. These results agreed well with those obtained in this study. Brettle *et al.*[2], Stamatakis *et al.*[8], and Vandre *et al.*[9] evaluated the DQE of the Digora system. The DQE spectrum of the Digora varied not only with exposure but with calibration setting. The maximal DQE in each spectrum ranged from 0.02 to 0.25. The value obtained in this study, approximately 0.09, was inside this range.

It is well known that both ST-V and HR-V are imaging plates used generally for medical radiography with the Fuji computed radiography system (Fuji Film Medical Co., Ltd., Tokyo, Japan). ST-V is used for general radiography. This IP has a high sensitivity to X-ray and standard resolution. HR-V is used for mammography and bone radiography. It has relatively low sensitivity to X-ray but high resolution. On the other hand, BAS-SR is an imaging plate not originally developed for imaging of human body but for autoradiography. Therefore resolution is more important than sensitivity to X-ray. The results of this study well reflected these characteristics of each IP.

In dental radiography, minute changes in bony structures should be depicted on the image. Therefore, NEQ and DQE at high spatial frequency become more important than those required for medical radiography. For this reason, we concluded that the HR-V has the best imaging properties for dental radiography among the three kinds of IPs evaluated in this study. Of course, each storage phosphor system is, without exception, designed to best utilize the properties of its IPs for optimal performance. However, the selection of the IP with the best imaging properties and a system designed to fully utilize the properties of that IP is essential for obtaining as much image information as possible at the lowest possible dosage to the patient.

There is one disadvantage with the HR-V. The light decay speed of image information was remarkably faster than with the BAS-SR. An IP with higher sensitivity to X-ray tended to show a faster light decay speed. To adopt the HR-V for a system such as the DenOptix, with which IPs are treated manually in an ordinary room[4], the light decay of image information should be taken into account. The best method under the present conditions is to treat the IP in a dim room. However, this method impedes simplicity of operation. More effective methods are expected.

REFERENCES

1) Borg, E., Attaelmanan, A. and Gröndahl, H.-G. (2000). Image plate systems differ in physical performance. *Oral Surg Oral Med Oral Pathol Oral Radiol Endod* **89**, 118–124.
2) Brettle, D.S., Workman, A., Ellwood, R.P., Launders, J.H., Horner, K. and Davies, R.M. (1996). The imaging performance of a storage phosphor system for dental radiography. *Brit J Radiol* **69**, 256–261.
3) Fujita, H., Tsai, D.-Y., Itoh, T., Doi, K., Morishita, J., Ueda, K. and Ohtsuka, A. (1992). A simple method for determining the modulation transfer function in digital radiography. *IEEE Trans Med Imaging* **MI-11**, 34–39.
4) Gendex Dental X-ray (Division of Dentsply International Corporation). (1997). *DenOptix user manual and installation guide,* Gendex Dental X-ray: USA.
5) Giger, M.L., Doi, K. and Fujita, H. (1986). Investigation of basic imaging properties in digital radiography. 7. Noise Wiener spectra of II-TV digital imaging systems. *Med Phys* **13**, 131–138.
6) Johns, H.E. and Cunningham, J.R. (1977). The Physics of Radiology. 3rd ed., pp. 735, Charles C Thomas, Springfield.

7) Nishikawa, K., Mori, T., Shibuya, H., Hayakawa, Y., Wakoh, M. and Kuroyanagi, K. (1999). Dose response of two storage-phosphor systems for intra-oral radiography. *Oral Radiol* **15**, 125–133.
8) Stamatakis, H.C., Welander, U. and McDavid, W.D. (2000). Physical properties of a photostimulable phosphor system for intra-oral radiography. *Dentomaxillofac Radiol* **29**, 28–34.
9) Vandre, R.H., Pajak, J.C., Abdel-Nabi, H., Farman, T.T. and Farman, A.G. (2000). Comparison of observer performance in determining the position of endodontic files with physical measures in the evaluation of dental X-ray imaging systems. *Dentomaxillofac Radiol* **29**, 216–222.

Reprint requests to:
Dr. Keiichi Nishikawa
Department of Oral and
Maxillofacial Radiology,
Tokyo Dental College,
1-2-2 Masago, Mihama-ku,
Chiba 261-8502, Japan